J Mater Sci: Mater Electron (2021) 32:25963–25972

Investigation of the microwave absorbing properties on polymer sheets

Monika Mishra[1], Avanish Pratap Singh[2,*], Manish Kumar[2], Tejendra Kumar Gupta[3], Hema Bhandari[4], and Mahesh Chand[5]

[1] *Department of Physics, Netaji Subhas University of Technology, Delhi 110 078, India*
[2] *Department of Physics, Atma Ram Sanatan Dharma College, University of Delhi, Delhi 110 021, India*
[3] *Amity Institute of Applied Sciences, Amity University, Sector-125, Noida, Uttar Pradesh 201313, India*
[4] *Department of Chemistry, Maitreyi College, University of Delhi, Delhi 110 021, India*
[5] *Faculty UnB Planaltina Campus, Nano Lab, Universidade de Brasılia, Brasılia, DF 73300-000, Brazil*

Received: 2 October 2020
Accepted: 4 February 2021
Published online: 4 March 2021

ABSTRACT

Electromagnetic (EM) absorbers are becoming an important tool in the recent advanced technologies as well as for environments to minimize the level of microwave radiations in specific structures or places. Indeed, they are employed in radar absorbing materials (RAMs) and in defense, communication electronics, medical equipment, human health care, laboratory environments and public safety issues. In strategic areas, where the electromagnetic interference (EMI) shielding effectiveness is essential, the components and parts made by EMI shielding materials is to be upgraded. The EM shield play a significant role in reducing the intensity of reflected and transmitted EM waves. Recently, research on EM wave absorbers is focused on polymer-based structures, and layered carbon structures. The basic qualities of polymer and carbon have been successfully applied to minimize the reflection coefficient, and maximize absorption coefficient in metrology as well as in defense equipment's. In this context, most of the studies use composites made with polymers and carbon materials and some studies are focused on foamed structures and metamaterials. In the present work, polyaniline (PANI) and carbon fiber (CF)-based paper like sheet structures were produced by compression molding technique and their electrical and EMI shielding properties are measured in X-band (8.2–12.4 GHz) frequency range. PANI paper has been found to have an electrical conductivity of 12.48 S/cm and EMI shielding effectiveness of PANI paper is found to be − 26.82 dB at a thickness of 0.75 mm. Scanning electron microscopy (SEM) approves the coating of polymer on carbon fiber and thermogravimetric analysis (TGA) demonstrates that the presence of carbon fiber drastically improves the thermal stability of the polymer sheets .

Address correspondence to E-mail: apsrajput@arsd.du.ac.in

https://doi.org/10.1007/s10854-021-05485-6

1 Introduction

For the past few decades, composites of intrinsically conducting polymers (ICPs) have attracted considerable attention due to their multifunctional character. These plastic metals have been proven as potential candidate for electromagnetic shielding, microwave absorbers, light-emitting diodes, biosensors, fuel and solar cells, antistatic packaging, and in electrochromic device due to their tunable conductivity that opens new prospective for polymers [1–3]. However, the wide use of these electro-polymerized ICPs or their free-standing thin films is limited due to poor mechanical performance [4]. Polyaniline (PANI) has emerged as one of the most promising ICP because of its ease of processing, environmental stability, light weight, low cost, and easy doping/dedoping chemistry [5, 6]. As compared to other ICPs, the electrical conductivity of neat PANI is as high as 100 S/cm but, similar to other ICP, PANI also have low mechanical strength but this issue can be overcome by the use of some proper binder and filler material which can impart strength to make it a free-standing conductive polymer composite. Carbon fibers (CFs) appear the most suitable candidate to be used as filler due to its low density and high mechanical strength [7]. Moreover, the high electrical conductivity of CF provides additional advantage to the PANI composites.

The flexibility, light weight, easy processing, and low cost make polymeric composites most suitable for packaging of sensitive electronic equipment and components like ICs, silicon wafers, medical equipment [8, 9]. However, the insulating characteristic of these polymers fails to dissipate static charges occurred on the surface which results in sparking especially at dry and hot weather conditions lead to malfunctioning of equipment. Therefore, optimum conductivity is required in packaging materials to continuously drain the charges from their surface. These conducting packaging materials can also suppress the undesired electromagnetic interference (EMI). In addition, by ensuring that all electronic devices are run with a good housing to prevent unnecessary radio frequency from entering or leaving, EMI can be removed. The major requirement for the household shielding is electrical conductivity. The incorporation of conducting fillers like metal and carbon-based materials to the polymers solves this purpose [10, 11]. However, the processing and uniform dispersion of these fillers is a great concern.

Wang et al. [12] has prepared metal organic framework derived yolk–shell Ni@C@ZnO microspheres, and the reflection loss was measured. They found the maximum reflection loss of -55.8 dB at 2.5 mm thickness. This enhancement in the microwave absorption is due to the interfacial polarization of Ni-C-ZnO, which contributes the metallic/semiconducting barriers. In a report of Wang et al. [13], core@shell structure CNTs@MoS_2 nanocomposites were synthesized by hydrothermal method and their microwave absorption properties were measured. The minimal reflection loss value of as prepared CNT@MoS_2 sample at 40 wt. % filler loading was found to be -54.75 dB at a thickness of 1.49 mm.

Saini et al. has synthesized PANI nanocomposites by in situ emulsion route with incorporation of different wt. % of graphite in to PANI matrix. The total EMI shielding value of -33.6 dB was measured in X-band frequency range (8.2–12.4 GHz) by incorporation of 15.6 wt.% of graphite in PANI matrix. In another investigation by Saini et al., colloidal graphite is used as reinforcement to improve the properties of PANI-based composite, it is demonstrated that 17.4 wt. % loading of colloidal graphite is able to enhance EMI-SE up to -39.7 dB in the X-band frequency region.

The addition of fly ash in PANI in a ratio of 3:1 has enhanced the EMI shielding of -32 dB in the X-band frequency range [14]. Incorporation of multiwalled carbon nanotubes (MWCNTs) in the PANI matrix by in situ polymerization process, the EMI shielding was increased up to -39 dB in the Ku-band frequency range at 25 wt. % loading of MWCNTs. In a study of Bingqing et al. [15], the PANI based nanocomposite were fabricated by incorporation of single wall carbon nanotubes (SWCNTs) and graphene, EMI shielding was measured separately for both the fillers. It is found that the addition of 25 wt.% of SWCNT and 33 wt. % of graphene sheets in PANI matrix, the total EMI-SE was found to be − 31.5 dB and − 34.2 dB, respectively. In all these above studies, the complex fabrication process and dispersion problems of carbon-based nanofillers in polymer matrix for microwave absorption applications are great challenging task for the researchers. Therefore, there is a need to look for new materials especially useful for microwave absorption properties that can help the research community.

Materials based on layered sheets have recently attracted great interest due to their many extraordinary properties [16]. In our present study, PANI/CF composite layered sheets/films have been fabricated using novalac phenol as binder material with a thickness of 0.25 mm. Chopped CF was used as substrate for deposition of conducting PANI. To provide better dispersion of CF in PANI, we use in situ polymerization technique. The SEM image of CF after deposition confirms that a layer of PANI is deposited on it. The EMI-SE of the films formed were measured by using single and multiple layers.

2 Experimental section

2.1 Materials used

Aniline was purchased from Loba Chemie, India and prior to use, aniline was purified by distillation process under reduced pressure. Carbon fiber (Toray T-300-Japan) was used as a reinforcement in PANI matrix to enhance the mechanical strength and phenol resin (Pheno-Organic, India) was used as a binder. The solvent used in the present study was methanol and ethanol purchased from Merck, India. Other chemicals such as ammonium peroxydisulfate (APS, Merck, India) and β- naphthalene-2-sulfonic acid (β-NSA, Himedia, India) used in this study are of reagent grade. Aqueous solutions were prepared using double distilled water of specific resistivity of 10^6 Ωcm.

2.2 Synthesis of PANI paper or polymer sheets

In order to prepare the pristine PANI and its composites, chemical oxidative polymerization of monomers was carried out. $\beta - NSA$ is used as the dopant and offers template for tubular growth of polymer [9]. in a standard preparation method for PANI sheets, 0.3 M $\beta - NSA$ solution and measured quantity of carbon fiber were homogenized for 3 h to obtain a uniform carbon fiber suspension. To form an emulsifier suspension, 0.1 M aniline was added and stirred continuously for at-least 1 h and cooled in an ice bath for another 2 h. Retaining the reactor temperature at 0 °C, the oxidant APS (0.1 M) was applied in drop by drop, with intense stirring. Finally, green polymer precipitate was collected and methanol treated to extract oligomers and washed several times with distilled water until the filtrate became colorless and then dried in a vacuum oven at 60–65 °C.

Thin paper or sheet like structure of PANI/carbon fiber was prepared using solution-based processing technique as illustrated in Scheme 1. Carbon fiber serves as a binding or filling substance in the polymer sheet, and phenol resin serves as a matrix. The concentration of carbon fiber and phenol resin is optimized elsewhere [7], The PANI-carbon fiber composite mixed in resin solution was then sonicated for two hours, homogenized for another 30 min, and then transferred into an especially built vessel to evaporate the solvent. Thin paper was then prepared at 130 °C using compression molding. The polymer sheets were then characterized for surface, electrical, and microwave shielding properties.

3 Results and discussion

The PANI-carbon fiber composite was prepared using aniline-carbon fiber as a dispersed phase in distilled water by the in-situ emulsion polymerization method. The amphiphilic nature of $\beta - NSA$ (with hydrophobic tail and the hydrophilic SO_3H head) preserves surfactant nature and produces micelles in aqueous solution. As pointed out in the experimental section, chopped carbon fiber of length $\sim$ 1 mm were dispersed in $\beta - NSA$ solution. As a consequence, micelles having $core - shell$ morphology were form during the reaction. In these micelles $\beta - NSA$ forms the "shell" while carbon fibers are resided in the "core". Monomer also reacts with β-NSA through an acid / base reaction to form a monomer / β-NSA salt. The micelles of aniline/β-NSA act as a soft template for polymer tubular growth [17]. The associated-SO3H group imparts β-NSA with additional dopant properties [9]. With advance of polymerization, the micelles containing carbon fiber will become larger cylinder. the above scheme suggests that through a self-assembly process, PANI and carbon fiber assemble polymer composite in cylinder like form.

3.1 Surface morphological analysis

SEM has been performed to view the distribution of carbon fiber in the polymer matrix. The SEM picture of pristine PANI synthesized in the presence of β-

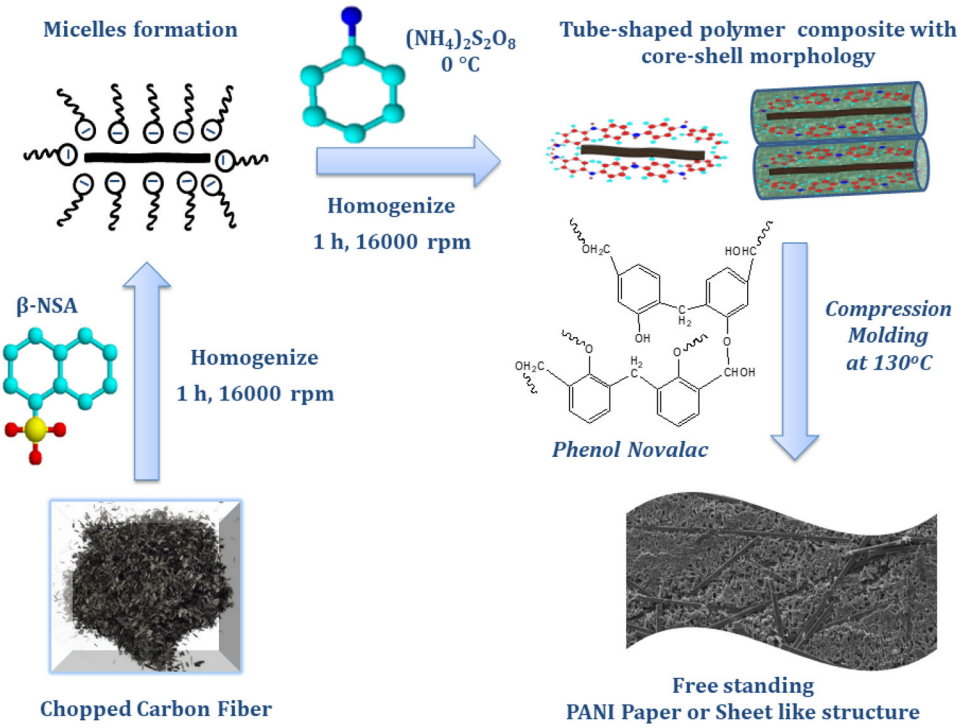

Scheme 1 Schematic representation of synthesis process of polymer paper using compression molding

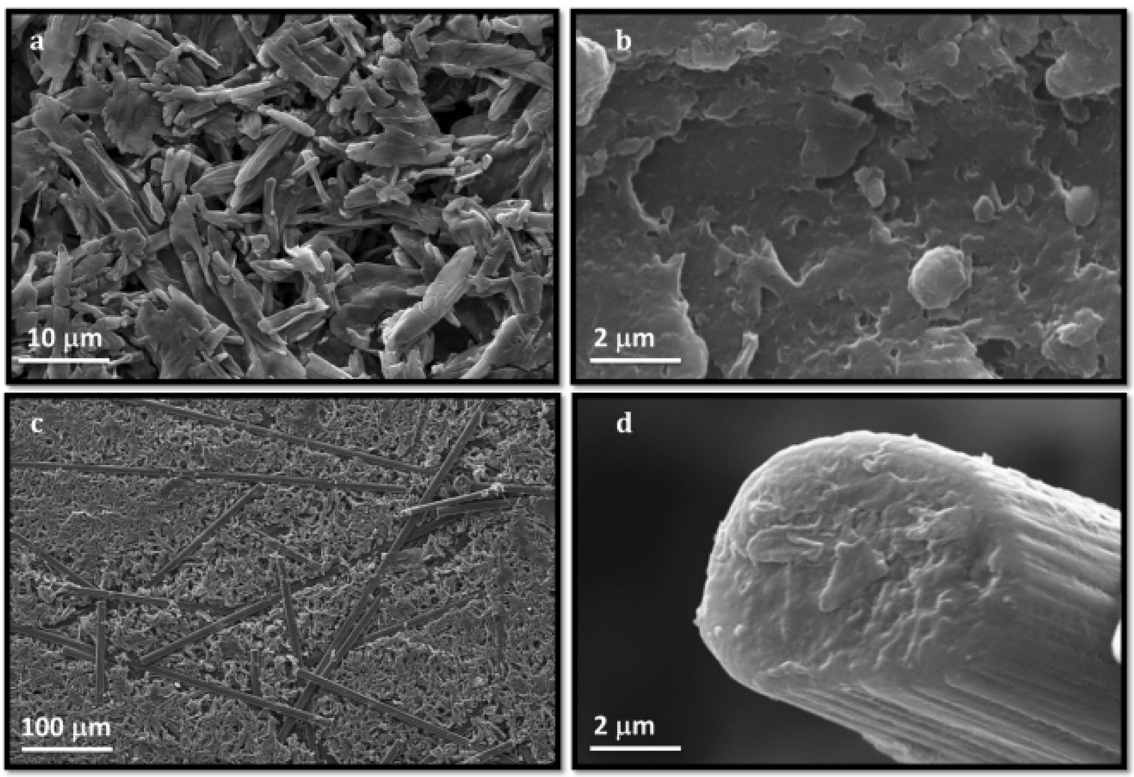

Fig. 1 SEM images of **a** pristine PANI, **b** zoom in image of PANI tube, **c** PANI paper, and **d** single strain of PANI coated carbon fiber, showing the formation of polymer upon the carbon fiber surface

NSA shows a fascinating cylinder-like structure (Fig. 1a). Figure 1b is recorded by zooming in Fig. 1a which shows the external rough surface of pristine PANI tubes. As shown in Fig. 1c, the approximate size of the chopped carbon fiber was found to be up to a few micrometers. The Fig. 1d shows the surface of polymer coated carbon fiber. The diameter as well as length of PANI-carbon fiber composite is greater than the PANI because carbon fiber supports the growth of polymer along the length of carbon fiber.

3.2 Transmission electron micrograph (TEM) analysis

Figure 2a and b shows TEM image of pristine PANI, the PANI tubes has a length and diameter 1 μm 15 μm, respectively. When a single tube is focused on TEM, PANI tube of diameter 0.5 μm and length 2.4 μm is visible as shown in Fig. 2b. We can conclude that PANI tubes has an average aspect ratio 15 μm. Figure 2c and d show the TEM image of PANI coated carbon fiber. From Fig. 2d, it is evident that the carbon fiber was covered with PANI, both the outline of carbon fiber and polymer can be clearly observed. It is further demonstrated that during the in situ polymerization the growth of polymer takes place on the carbon fiber surface. Therefore, in the case of composite, the length of tubes depends on the carbon fiber's length. The coating thickness of polymer on carbon fibers is in even manner. Furthermore, the whole surface area of the carbon fiber is covered with polymer. Besides this, polymer coating is very strongly adhesive on carbon fiber: even sonication applied during TEM specimen's preparation, was not able to separate this coating from carbon fiber.

3.3 XRD analysis

Figure 3 shows the carbon fiber, pristine PANI, and PANI paper XRD patterns. The key carbon fiber peaks are centred at $2\theta = 26.265°$ corresponding to the (002) planes. The peaks at 43° are attributable to the graphitic planes (110) and (100) and small quantities of catalyst particles encapsulated within the walls of the carbon fiber. PANI exhibits two broad peaks at $2\theta = 19.795°$ ($d = 4.481$ Å) and 25.154° ($d = 3.537$ Å), indicating that it is amorphous [9]. The characteristic peaks of carbon fiber are present in

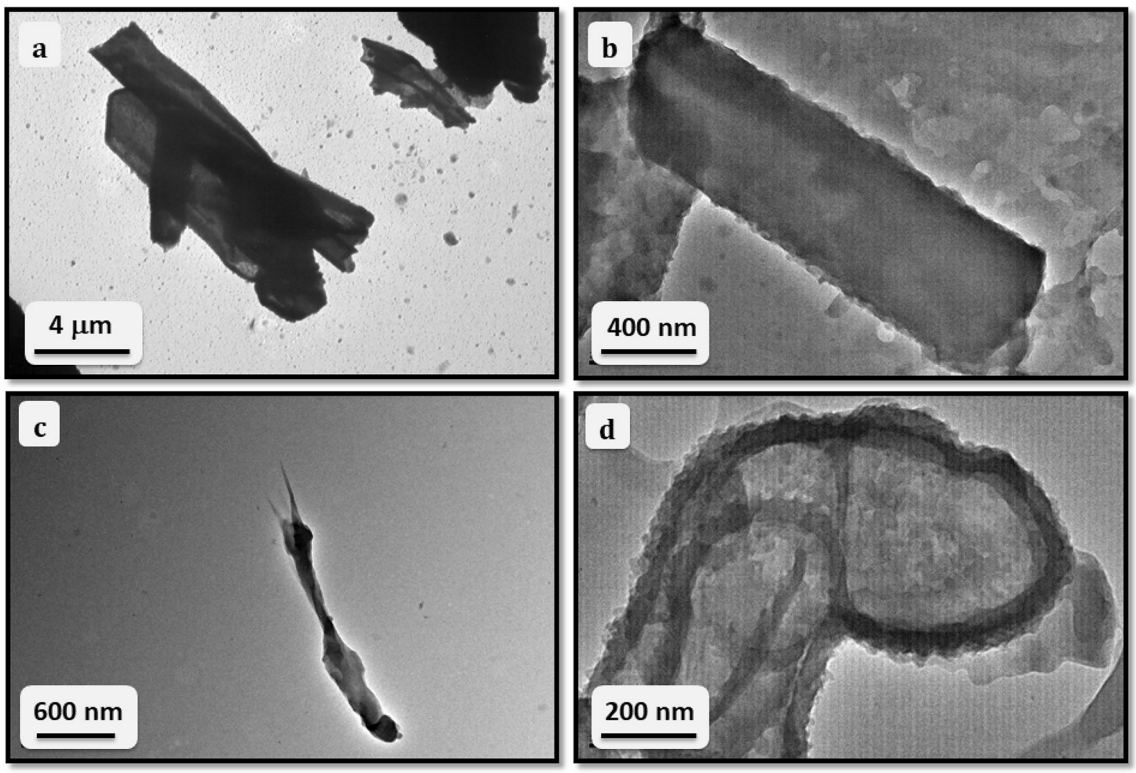

Fig. 2 TEM images of **a** pristine PANI, **b** zoom in image of PANI tube, **c** PANI-carbon fiber composite and **d** PANI coated carbon fiber, showing the presence of polymer on the carbon fiber surface

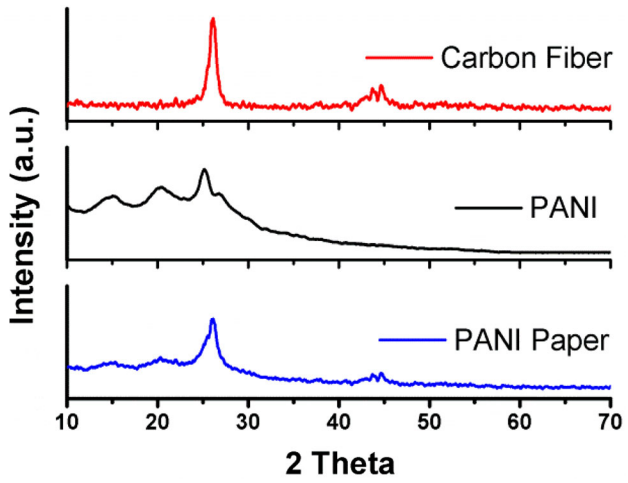

Fig. 3 XRD of carbon fiber, pristine PANI, and PANI paper

PANI paper, indicating that carbon fiber is present in PANI paper.

3.4 TGA analysis

To determine the effect of carbon fiber presence on the thermal stability of the Polymer sheet, perform thermogravimetric analysis (TGA) on the pristine PANI, carbon fiber, PANI-carbon fiber composite material and PANI paper (Fig. 4). PANI is thermally stable up to 270 °C with a weight loss of only 2%. The PANI and its paper show several stages of weight loss corresponding to loss of various components. The first step loss at 120 °C is the loss of volatile components like water. The second loss in the range of 270–350 °C is due to the loss of dopant $-SO_3H$ functional group and the onset of polymer degradation. The last major loss step (380° to 700 °C) is due to the complete decomposition of dopant and the polymeric backbone. When the decomposition reaction initially starts, the initial decomposition temperature (IDT) is also affected by carbon fiber absorption. The doped PANI has been shown to be thermally stable up to 255 °C (only 4% wt. loss). However, incorporating conductive carbon fiber into the PANI matrix can improve the thermal stability by 20 °C of the polymer. PANI paper is thermally stable up-to 275 °C. This shows the aniline's in situ polymerization in the presence of carbon fiber produces a better thermally stable conductive polymer.

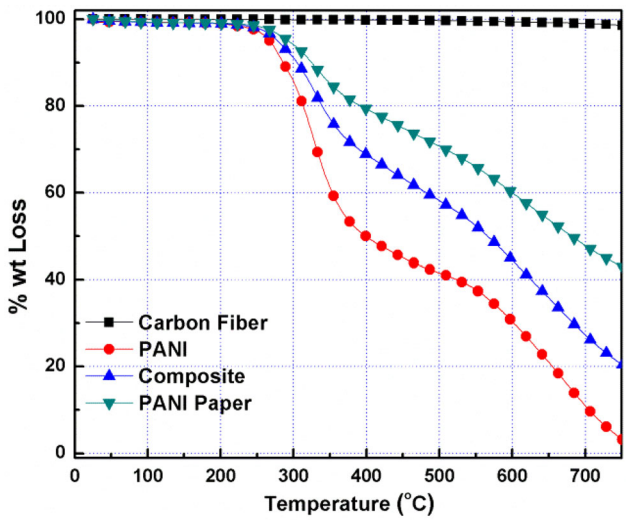

Fig. 4 Thermogravimetric (TG) plots of carbon fiber, PANI, and its composite and PANI paper in N_2 atmosphere

3.5 Electromagnetic interference shielding analysis

The logarithmic ratio of radiated input power (P_i) to output power (P_t) of radiation is known as EMI-SE. Usually, the efficacy of shielding materials is expressed in decibels (dB). The higher the EMI shielding effect's decibel level, the less energy can move through the shield. It relies on three variables [18–20]:

(a) Absorption: The shielding layer absorbs the wave.

(b) Reflection: The wave is mirrored from the front surface of the shielding material.

(c) Multiple reflections: reflections of waves from different shield-based interfaces.

Absolute efficiency of EMI shielding could therefore be expressed as [17, 21–25]

$$SE_T\,(dB) = SE_A + SE_R + SE_M = 10\log_{10}\left(\frac{P_t}{P_i}\right) \quad (1)$$

If the material 's overall EMI shielding performance reaches 10 dB, the multiple reflection loss (SE_M) can be ignored [18, 26, 27]. Therefore, total shielding effectiveness (SE_T) can be stated as

$$SE_T\,(dB) = SE_A + SE_R \quad (2)$$

"The Reflectance and transmittance can be connected to the scattering parameters S_{11} (or S_{22}) and S_{21} (or S_{12}) of a two port network analyzer as;

$R = |E_R/E_I|^2 = |S_{11}|^2 = |S_{22}|^2$ and.

$T = |E_T/E_I|^2 = |S_{21}|^2 = |S_{12}|^2$.

The absorbance (A) can be defined as, $A = (1 - R - T)$.

Here, the absorption coefficient is calculated with reference to the incident EM wave power. After first reflection, the relative strength of the effective incident EM wave inside the materials is dependent on the quantity (1-R). The effective absorbance (A_{eff}) can therefore, be defined as $A_{eff} = (1 - R - T)/(1 - R)$ in relation to the power of the effective incident EM wave inside the shield. The reflection and effective absorption losses are; therefore, conveniently expressed as; $10log_{10}(1 - R)$ and $-10log_{10}(1 - A_{eff})$, respectively, giving SE_A and SE_R as [28]:

$$SE_A = -10\log(1 - A_{eff}) = -10\log(T/1 - R)\, and\, SE_R = -10\log(1 - R)$$

Figure 5 shows the changes of the SE_A, SE_R, and SE_T in the frequency range 8.2–12.4 GHz range. SE is analyzed by varying thickness of the shield. For this purpose, 3 samples of the groove size were cut from the paper having average thickness 0.25 mm. Experimental measurements show that the absorption shielding effectiveness (SE_A) is 11.64 dB (0.25 mm), 15.54 dB (0.50 mm) and 19.91 dB (0.75 mm). That shows the absorption power of the PANI paper increases with increase in the thickness of the paper. Although the SE_R values remains constant around 8 dB at 10.2 GHz, with increase in the shield thickness as shown in Fig. 5. Thus, the total SE_T achieved for the PANI paper is 19.09 dB (0.25 mm) 22.76 dB (0.5 mm) 26.82 dB (0.75 mm) which is greater than the pristine PANI [9]. Therefore, it is established that in PANI paper, shielding effectiveness (SE) is conquered predominantly by absorption rather than reflection (SE_R). The observed SE is attributed to the electronic, ionic, orientation and space charge polarization rises in the shield when radiation incident on the shield. Owing to the presence of bound loads (dipoles), orientation polarization occurs. The heterogeneity of the shield contributes to the space charge polarization. Table 1 compares the electromagnetic shielding properties of similar PANI/Carbon fiber composites reported in the literature.

In PANI paper, two types of charged species occur in which first type of charged species are polaron and bipolaron that can move freely along the chains in polymer assembly. Second types of charged species are the bound charges (dipoles) which limits the mobility and explains the strong polarization within the system. When radiation enters the shielding layer, the dipoles cannot be reoriented again as easily as the electric field applied in the shield, which creates space charges on the uneven interface and distorts the electric field. The contribution of carbon fiber to ionic conduction becomes more pronounced at a low frequency of the applied electric field. Multiple

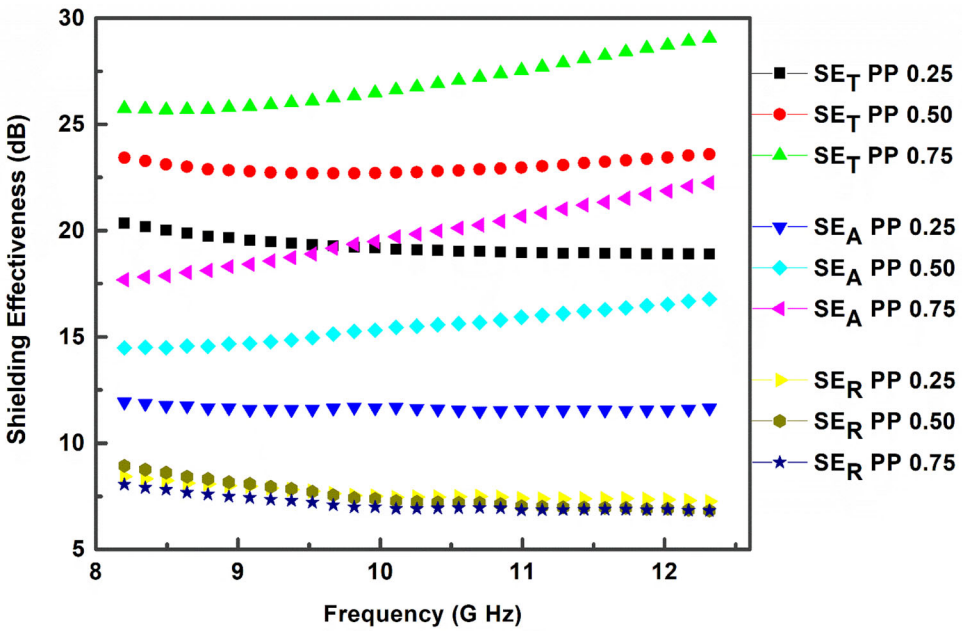

Fig. 5 EMI-SE graph of PANI paper as a variation with thickness

Table 1 Electromagnetic shielding properties of similar PANI/Carbon fiber composites

Sample details	Frequency Range (GHz)	Shielding Performance (dB)	References/Journal/Year
Artificial suede-like cloth (ASC) /PANI composite fabrics	8.2–12.4	25.9	Pan et.al. [29]/Composites Science and Technology/2020
Ba-Pb-Hexaferrite-Polyaniline-Wax Nanocomposites	18	15	Chaudhary et.al. [30]/Journal of Electronic Materials/2020
Aerogels of V2O5 nanowires reinforced by polyaniline	8.2–12.4	34	Narayanan et.al. [31]/Chemical Engineering Journal/2021
hybrid carbon nanotube reinforced polyaniline nanocomposites	12.4–18	57	Kumar et.al. [32]/Polymer-Plastics Technology and Engineering/2018
One-dimensional bagasse Fiber/Polyaniline Heterostructure	10	33.83	Zhang et.al. [33]/*ACS Appl. Polym. Mater.*/2019
Brick/polyaniline nanocomposite	8.2	7	Peymanfar et.al. [34]/Construction and Building Materials/2020
Polyaniline-carbon fiber thin sheets	12.4	31.9	Joon et.al. [35]/Materials Chemistry and Physics, (2015)
Polyaniline (PANI)-based vapor grown carbon fiber (VGCF-H) hybrid nanocomposite	8.2–12.4	51	Kumar et.al. [36]/Polym Eng Sci/2019
MWCNT/ polyurethane composite with a thickness of 1.5 mm	8.2–12.4	29	Gupta et.al. [37]/Journal of Polymer Research/2013
Polyaniline coated carbon nanotubes on fabrics nanocomposite	4 – 6	23	Zou et.al. [38]/Diamond and Related Materials/2020
PANI-Carbon Fiber Composite paper (0.75 mm)	8–12	29	Present study

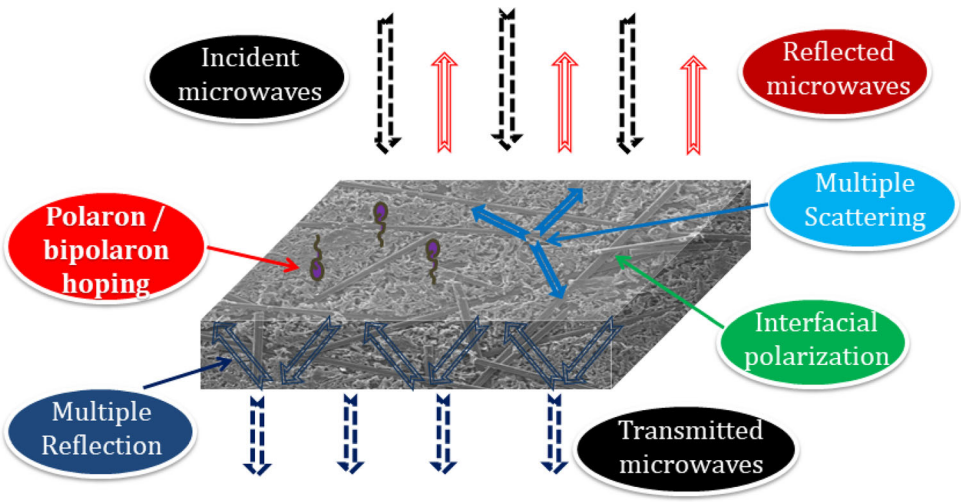

Fig. 6 Schematic representation of possible microwave shielding mechanism in polymer sheets

scattering plays an important role in improving microwave absorption. The moderate value of conductivity of PANI paper also effectively contributes in the enhancement of shielding effectiveness. Shielding mechanism of free-standing PANI paper is clearly demonstrated in Fig. 6.

4 Conclusion

Tubular shape PANI and PANI coated carbon fiber composite sheet have been synthesized by in situ chemical oxidative polymerization followed by compression molding at a temperature of 130 °C in the form of thin paper or sheet structure. The

synthesized thin composite paper is further characterized using SEM, XRD and TGA techniques. The outcome of the works shows that this unique carbon polymer structure can effectively improve the interfacial polarization, electronic polarization, and anisotropy properties during activation via microwaves. The three-layer PANI paper in which each layer has thickness of 0.25 mm focuses on the absorption component of EMI shielding rather than the reflection. The maximum value of EMI shielding due to absorption of -26.82 dB is achieved. Therefore, inclusion of carbon fiber in PANI matrix is very useful for improving the absorption component in X-band frequency range (8.2–12.4 GHz) as compared to the traditional materials. In addition, the shielding effect can easily be adjusted by changing the thickness of the sample. This indigenously developed material could potentially be useful in the microwave absorbing region .

Acknowledgements

The authors would like to thank Dr. S. K. Dhawan, Emeritus Scientist of the CSIR-National Physical Laboratory, New Delhi, India for his valuable comments and suggestions. One of the authors, M. Mishra is grateful to UGC, Govt. of India for providing the research grant under UGC Dr D.S. Kothari Post-Doctoral Fellowship Scheme.

References

1. Z. Zeng, Small. (2017). https://doi.org/10.1002/smll.201701388
2. S.K. Dhawan, N. Singh, D. Rodrigues, Sci. Technol. Adv. Mater **4**, 8 (2003)
3. P. Sambyal, A.P. Singh, M. Verma, M. Farukh, B.P. Singh, S.K. Dhawan, RSC Advances. (2014). https://doi.org/10.1039/c3ra46479b
4. N.H. Hoang, J.L. Wojkiewicz, J.L. Miane, R.S. Biscarro, Polym Adv Technol. (2007). https://doi.org/10.1016/j.carbon.2011.01.055
5. S. Goswami, U.N. Maiti, S. Maiti, S. Nandy, M.K. Mitra, K.K. Chattopadhyay, Carbon **49**, 2245 (2011)
6. M. Mishra, A.P. Singh, V. Gupta, A. Chandra, S.K. Dhawan, J. Alloy. Compd. (2016). https://doi.org/10.1016/j.jallcom.2016.07.190
7. A.P. Singh, P. Garg, F. Alam et al., Carbon **50**, 3868 (2012)
8. D.-W. Wang, F. Li, J. Zhao et al., ACS Nano **3**, 1745 (2009). https://doi.org/10.1021/nn900297m
9. A.P. Singh, S.A. Kumar, A. Chandra, S.K. Dhawan, AIP Adv. (2011). https://doi.org/10.1063/1.3608052
10. S.W. Phang, T. Hino, M.H. Abdullah, N. Karamoto, Mater. Chem. Phys **104**, 327–335 (2007)
11. W.-L. Song, M.-S. Cao, M.-M. Lu et al., Carbon **66**, 67 (2014). https://doi.org/10.1016/j.carbon.2013.08.043
12. L. Wang, X. Yu, X. Li, J. Zhang, M. Wang, R. Che, Chem. Eng. J. **383**, 123099 (2020)
13. R. Wang, E. Yang, X. Qi et al., Appl. Surf. Sci. (2020). https://doi.org/10.1016/j.apsusc.2020.146159
14. A.P. Singh, A. Chandra, S. Dhawan, AIP Adv. **1**, 022147 (2011)
15. B. Yuan, L. Yu, L. Sheng, K. An, X. Zhao, J. Phys. D Appl. Phys. **45**, 235108 (2012)
16. T.K. Gupta, B.P. Singh, V.N. Singh et al., Journal of Materials Chemistry A **2**, 4256 (2014)
17. A.P. Singh, M. Mishra, P. Sambyal et al., Journal of Materials Chemistry A. (2013). https://doi.org/10.1039/c3ta14212d
18. T.K. Gupta, B.P. Singh, S.R. Dhakate, V.N. Singh, R.B. Mathur, Journal of Materials Chemistry A. (2013). https://doi.org/10.1039/c3ta11611e
19. R. Kumar, S.R. Dhakate, T. Gupta, P. Saini, B.P. Singh, R.B. Mathur, Journal of Materials Chemistry A **1**, 5727 (2013). https://doi.org/10.1039/c3ta10604g
20. M. Wu, A.K. Darboe, X. Qi et al., Journal of Materials Chemistry C **8**, 11936 (2020). https://doi.org/10.1039/D0TC01970D
21. B.P. SinghP Saini et al., J. Nanopart. Res. (2011). https://doi.org/10.1007/s11051-011-0619-1
22. T.K. Gupta, B.P. Singh, S. Teotia, V. Katyal, S.R. Dhakate, R.B. Mathur, J Polym Res **20**, 1 (2013). https://doi.org/10.1007/s10965-013-0169-6
23. H.-B. Zhang, Q. Yan, W.-G. Zheng, Z. He, Z.-Z. Yu, ACS Appl. Mater. Interfaces. **3**, 918 (2011). https://doi.org/10.1021/am200021v
24. A.P. Singh, M. Mishra, A. Chandra, S.K. Dhawan, Nanotechnology **22**, 9 (2011)
25. B.P. Singh, V. Choudhary et al., J Nanopart Res (2013). https://doi.org/10.1007/s11051-013-1554-0
26. K. Singh, A. Ohlan, V.H. Pham et al., Nanoscale **5**, 2411 (2013). https://doi.org/10.1039/c3nr33962a
27. A. Ohlan, K. Singh, A. Chandra, S.K. Dhawan, ACS Appl. Mater. Interfaces. **2**, 927 (2010). https://doi.org/10.1021/am900893d
28. A.P. Singh, M. Mishra, S. Dhawan, *Conducting Multiphase Magnetic Nanocomposites for Microwave Shielding Application; "Nanomagnetism"* (One Central Press, UK, 2015).

29. T. Pan, Y. Zhang, C. Wang, H. Gao, B. Wen, B. Yao, Compos. Sci. Technol. **188**, 107991 (2020). https://doi.org/10.1016/j.compscitech.2020.107991
30. H.K. Choudhary, R. Kumar, S.P. Pawar, S. Bose, B. Sahoo, J. Electron. Mater. **49**, 1618 (2020). https://doi.org/10.1007/s11664-019-07478-y
31. A.P. Narayanan, K.N.N. Unni, K.P. Surendran, Chem. Eng. J. (2021). https://doi.org/10.1016/j.cej.2020.127239
32. A. Kumar, V. Kumar, K. Awasthi, Polymer-Plastics Technology and Engineering **57**, 70 (2018). https://doi.org/10.1080/03602559.2017.1300817
33. Y. Zhang, Z. Yang, Y. Yu, B. Wen, Y. Liu, M. Qiu, ACS Applied Polymer Materials **1**, 737 (2019). https://doi.org/10.1021/acsapm.8b00025
34. R. Peymanfar, S. Keykavous-Amand, M.M. Abadi, Y. Yassi, Constr. Build. Mater. **263**, 120042 (2020). https://doi.org/10.1016/j.conbuildmat.2020.120042
35. S. Joon, R. Kumar, A.P. Singh, R. Shukla, S.K. Dhawan, Mater. Chem. Phys. **160**, 87 (2015). https://doi.org/10.1016/j.matchemphys.2015.04.010
36. V. Kumar, M.A. Muflikhun, T Yokozeki **59**, 956 (2019). https://doi.org/10.1002/pen.25045
37. T. Gupta, B. Singh, S. Teotia, V. Katyal, S. Dhakate, R. Mathur, J. Polym. Res. **20**, 169 (2013)
38. L. Zou, C. Lan, L. Yang et al., Diam. Relat. Mater. **104**, 107757 (2020). https://doi.org/10.1016/j.diamond.2020.107757